Am J Transl Res 2019;11(5):2668-2682
www.ajtr.org /ISSN:1943-8141/AJTR0091835

Original Article

Berberine prevents non-alcoholic steatohepatitis-derived hepatocellular carcinoma by inhibiting inflammation and angiogenesis in mice

Yan Luo[1,2], Guoyan Tian[3], Zhenjie Zhuang[2], Jin Chen[6], Ningning You[7], Lili Zhuo[7], Bingtian Liang[6], Yu Song[7], Shufei Zang[4,8], Juan Liu[5], Jin Yang[2], Weihong Ge[1], Junping Shi[2]

[1]College of Pharmaceutical Science, Zhejiang Chinese Medical University, Hangzhou, Zhejiang, China; [2]Institute of Translational Medicine, Departments of [3]Oncology and Hematology, [4]Endocrinology, [5]Pathology, The Affiliated Hospital of Hangzhou Normal University, Hangzhou, Zhejiang, China; [6]Fourth Clinical Medicine College, Zhejiang Chinese Medical University, Hangzhou, Zhejiang, China; [7]Hangzhou Normal University, Hangzhou, Zhejiang, China; [8]Department of Endocrinology, Shanghai Fifth People's Hospital Affiliated to Fudan University, Shanghai, China

Received January 25, 2019; Accepted April 25, 2019; Epub May 15, 2019; Published May 30, 2019

Abstract: Hepatocellular carcinoma (HCC) is one of the most malignant and poor prognosis tumors, which was increasingly caused by nonalcoholic fatty liver disease/nonalcoholic steatohepatitis (NAFLD/NASH) in western countries. In this study, we aimed to investigate the mechanism and therapeutic prospect of berberine in the treatment of NASH-HCC mice. Combination of STZ injection and high fat and high-cholesterol diet (HFHC) was used to establish NASH-HCC model. The effect of berberine intervention is studied from histology, biochemistry and molecular level. Our results showed that administration of berberine to NASH-HCC mice reduced the incidence of tumors and mitigated NASH. Berberine significantly reduced the levels of alanine aminotransferase (ALT), aspartate aminotransferase (AST), glucose (GLU), high-density lipoprotein (HDL), low-density lipoprotein (LDL) and total cholesterol (TC). Transcriptome sequencing and bioinformatics analysis identified numberous genes and various pathways may participate in the favorite effect of berberine. Specifically, berberine suppressed the expressions of genes related to lipogenesis, inflammation, fibrosis and angiogenesis. Moreover, our results showed that berberine suppressed phosphorylation of p38MAPK and ERK as well as COX2 expression significantly. This suggested berberine achieved its biological functions mainly by regulating inflammation and angiogenesis genes involving p38MAPK/ERK-COX2 pathways. This study demonstrated the anti-tumor effects of berberine and its possible mechanism, providing a potential drug for treating NASH-HCC.

Keywords: Berberine, NASH, HCC, inflammation, angiogenesis

Introduction

Hepatocellular carcinoma (HCC) is the most common type of primary liver cancer and the second leading cause of solid tumor death worldwide [1]. Non-alcoholic fatty liver disease (NAFLD) is a clinical syndrome characterized by hepatocyte steatosis and lipid accumulation, which is caused by metabolic factors, excluding alcohol consumption and other definite liver-damaging factors. The disease spectrum includes simple fatty liver and the evolved steatohepatitis (NASH), cirrhosis and HCC. With the development of economy and the change of people's diet and lifestyle, NAFLD, as a liver complication of metabolic syndrome such as obesity and diabetes, has become the fastest growing and most important cause of HCC in developed countries. The global incidence of NAFLD was 25% [2]. NASH is the progressive form of NAFLD and a key link in the development of liver fibrosis, cirrhosis and even liver cancer. Due to the increasing prevalence and growth rate of NAFLD, the incidence of NASH-derived HCC is also on the rise. NASH-HCC is more insidious and progresses more rapidly than viral hepatitis-related HCC, with larger tumors and poorer prognosis [3, 4]. Currently, there is still a lack of effective drugs for NASH treatment in clinical practice, not to mention

the means and indicators to prevent and monitor the progression of NASH into HCC. Therefore, it is of great practical significance to strengthen the study on the mechanism of NASH-HCC and search for effective drugs for the prevention and treatment of NASH-HCC.

Berberine, as the active component of Coptis chinensis, is often used in clinical treatment of acute gastroenteritis, and has been used in the treatment of digestive tract diseases in China for thousands of years [5]. In recent years, studies have found that berberine can promote the browning of adipose tissue and enhance the energy consumption of the body by enhancing the autophagy effect of liver Sirt1 and upregulating the expression of FGF21, thereby down-regulating the level of lipid deposition and improving fatty liver [6]. At the same time, studies have found that berberine has broad-spectrum antibacterial and anti-tumor effects, and has certain inhibitory and killing effects on liver cancer, colon cancer, lung cancer, breast cancer, melanoma, neuroblastoma and other tumor cells [7-12]. Berberine can kill tumor cells by inhibiting protein synthesis of cancer cells, inducing cell cycle arrest in G2/M phase and promoting apoptosis of liver cancer cells [13, 14]. Although berberine has been reported to have a mutiple anti-tumor effect, these data mainly come from in vitro experimental studies on liver cancer cells and nude mice, and there is no literature on the overall study on the efficacy and pharmacological effects of berberine in the animal model of NASH-HCC. Recently, researchers have reported that streptozotocin (STZ) injection with a high-fat diet can develop a NASH-HCC mouse model [15], which is able to reflect a pathological process developing from fatty liver, steatohepatitis and fibrosis to HCC. In this study, we aimed to investigate the pharmacological effect and the underline mechanism of berberine on NASH-HCC induced by high fat and high cholesterol diet combined with streptozotocin injection in mice.

Materials and methods

Animals and treatments

The C57BL/6J mice (10 males and 20 females, 8-10 weeks) were purchased from SLAC Laboratory Animal Co., Ltd. (Shanghai, China). The animals were kept in a room with a 12 hours light/dark cycle at 22°C (humidity: 40%-70%; luminosity: natural lighting). The mice were given free access to food and water. The animals were mated and the new born animals (3-4 days) were subcutaneously injected with STZ (2 mg/ml stock solution, 0.1 ml per mouse; Cat. S0130, Sigma, St Louis, MI, USA). After weaning (5 weeks after born), these animals received STZ injection were initially randomized into three groups. One group (n = 10, male) was fed with normal chow diet. One group (n = 10, male) was fed with high fat and high-cholesterol diet (HFHC, Cat. D12079B, Research Diet, New Brunswick, NJ) to generate NASH-HCC according to previous studies [16, 17]; another group (n = 10, male), after being fed with HFHC and the mice were also treated with berberine (Cat. B3251, Sigma, St Louis, MI, USA) gavage (250 mg/kg) everyday as previously described [18, 19]. These three groups were respectively fed with corresponding diet for 12 weeks. The body weight of the animals was recorded. At the end of experiments, all the animals were anesthetized with 40 mg/kg pentobarbital Na (Sigma-Aldrich, Merck KGaA). The blood was collected and liver was obtained then weighed. The serum was collected by centrifuging at 1000 g for 10 min. The supernatant was obtained for determining ALT, AST, GLU, HDL, LDL and TC in the serum. All experiments were approved by the Institutional Animal Care and Use Committee of The Affiliated Hospital of Hangzhou Normal University (2016 03A1X, Hangzhou, China).

RNA extraction and transcriptome sequencing

Total RNA of liver tissues was isolated using TRIzol following the protocol (15596018, Invitrogen, San Diego, CA, USA). Briefly, liver tissues were homogenized in 1000 μL Trizol reagent followed by 200 μL chloroform. Next, the samples were vortexed for 5 min. After centrifugation (12,000 g for 15 min at 4°C), the supernatant was carefully drawn into a new tube. Equal volume of isopropyl alcohol was added and incubated at room temperature for 20 min. Following the centrifugation (12,000 g at 4°C for 10 min), the supernatants were removed completely and the precipitate was washed twice by 75% ethanol. Finally, nuclease-free water was added to elute the RNA. The concentration and purity were detected using e-spect Fluorescent spectrophotometer (Malcom, Japan).

The quantification and qualification of extracted RNA was assessed using the RNA Nano 6000 Assay Kit (5067-1511, Agilent Technologies, CA, USA) of the Bioanalyzer 2100 system (Agilent Technologies, CA, USA). The NEBNext Ultra TM RNA Library PrepKit for Illumina (E7530S, New England Biolabs, USA) was used to generate sequencing libraries. Briefly, mRNA was purified using poly-T oligo attached magnetic beads, and then randomly fragmented by bivalent cation in the NEB Fragmentation Buffer. The fragment mRNA was used as template to synthesize the first strand cDNA using radom hexamer primer and M-MuLV reverse transcriptase. The second strand of cDNA was subsequently synthesized using DNA polymerase and RNase H. After purification, remaining overhangs were repaired, 3'ends of the DNA fragments were adenylated, and NEBNext Adaptor with hairpin loop structure were ligated to prepare for hybridization. AMPure XP system (Beckman Coulter, Beverly, USA) were used to select cDNA fragments of preferentially 250-300 bp in length. PCR amplification was performed and the PCR products were purified using AMPure XP system again. Library quality was assessed on the Agilent Bioanalyzer 2100 system. The library preparations were sequenced on Illumina HiSeq platform with the sequencing read length of 125/150 bp. RNA-Seq data were produced by Beijing Novegene Bioinformatics Technology Co., Ltd. (Beijing, China).

Functional and pathway enrichment analysis

Sequencing data were analyzed and the differentially expressed genes (DEGs) were represented with a Venn Diagram (http://bioinfogp.cnb.csic.es/tools/venny/index.html;Venny2.1.0). Furthermore, the Database for Annotation, Visualization and Integrated Discovery (http://www.david.abcc.ncifcrf. gov) provided a complete set of functional annotation tools to help identify the targets in gene lists that may be associated with the biological problems in question. Besides, these DEGs can be analyzed by Gene Ontology (Go) function and Kyoto Encyclopedia of Genes and Genomes (KEGG) pathway enrichment analysis with DAVID online analysis (*P*-value was set to 0.05).

Biochemical analysis

Serum levels of ALT, AST, GLU, HDL, LDL and TC were measured by using a Hitachi automatic analyzer 7600 (Tokyo, Japan) according to the manufactures' protocols.

Histological analysis

The liver tissue morphology and liver fibrosis were evaluated using HE staining and Masson staining. Masson Trichrome staining was performed following the protocol (Cat. G1006, Servicebio, Wuhan, China). Briefly, sections were fixed in Bouin's Solution. They were then stained in Weigert's iron hematoxylin solution for 5 min between washes. After the sections were incubated in Biebrich Scarlet, they were then set in phosphotungstic/phosphomolybdic acid solution for 5 min. Next, the sections were set in aniline blue for 5 min. Finally, the sections were fixed using 1% acetic acid for 1 min. The histological analysis for Nonalcoholic steatohepatitis (NASH) was according to NAS system developed by clinical research network [20], hepatic steatosis (0-3), inflammation (0-3), hepatocyte ballooning (0-2). Liver tissues were fixed in formaldehyde and then blocked in paraffin. Next, sections were stained with hematoxylin for 5 min followed by staining with eosin for 3 min (Cat. G1005, Servicebio, Wuhan, China). Oil Red O (Cat. 00625, Sigma, St Louis, MI, USA) was used to stain lipids in the liver. Briefly, the sections were firstly fixed with 10% formaldehyde and washed by water and 60% isopropanol, then stained with Oil Red O working solution (in 0.18% isopropanol) for 20 min and washed by 60% isopropanol. Nuclei were stained with hematoxylin.

Immunohistochemistry analysis

Liver sections of mice were prepared for immunostaining using anti CD31 (1:100, Cat. GB-11063, Servicebio), anti-CD34 (1:500, Cat. GB-13013, Servicebio), anti-VEGF (1:200, Cat. GB11034, Servicebio), anti-COX2 (1:250, Cat. ab179800, Abcam), anti-CD68 (1:200, Cat. ab125212, Abcam) and anti-F4/80 (1:200, Cat. 70076s, Cell Signaling Technology) antibodies according to the manufacturer's instructions. Vascular endothelial cells with prominent staining and be separated from adjacent blood vessels, tumor cells, and interstitial components are considered as countable blood vessel. The membranous and cytoplasmic granular staining with VEGF was determined for all tumor cells. For each section, positive and negative

Table 1. Primer sequences for qPCR analysis

Gene name	Forward (5'-3')	Reverse (5'-3')
GAPDH	AGGTCGGTGTGAACGGATTTG	TGTAGACCATGTAGTTGAGGTCA
FASN	GGAGGTGGTGATAGCCGGTAT	TGGGTAATCCATAGAGCCCAG
SCD1	ACTGTGGAGACGTGTTCTGGA	ACGGGTGTCTGGTAGACCTC
SREBP1C	TGACCCGGCTATTCCGTGA	CTGGGCTGAGCAATACAGTTC
COL1A1	GCTCCTCTTAGGGGCCACT	CCACGTCTCACCATTGGGG
TIMP-1	GCAACTCGGACCTGGTCATAA	CGGCCCGTGATGAGAAACT
a-SMA	GTCCCAGACATCAGGGAGTAA	TCGGATACTTCAGCGTCAGGA
VEGFR	TTTGGCAAATACAACCCTTCAGA	GCAGAAGATACTGTCACCACC
CD31	GAGCCCAATCACGTTTCAGTTT	TCCTTCCTGCTTCTTGCTAGCT
MCP-1	TCCCAATGAGTAGGCTGGAG	TCTGGACCCATTCCTTCTTG
TNF-α	AAGGGAGAGTGGTCAGGTTG	TCTGTGAGGAAGGCTGTGC
CD68	TCCAAGATCCTCCACTGTTG	ATTTGAATTTGGGCTTGGAG
IL-1β	CCCAAGCAATACCCAAAGAA	GCTTGTGCTCTGCTTGTGAG
F4/80	TAGTGGAGGCAGTGATGCTC	TATGACCACCAGGACTGGAA
IL6	AGAAGGAGTGGCTAAGGACCAA	AACGCACTAGGTTTGCCGAGTA
COX2	AACCGCATTGCCTCTGAAT	CATGTTCCAGGAGGATGGAG

controls for each marker were established. As a negative control, liver tissue section was incubated with PBS lack of primary antibody. The positive control section was provided by the suppliers. Image-Pro Plus 6.0 was used to analyze the value of integrated optical density (IOD).

Reverse transcription and quantitative real-time PCR (qPCR)

Total RNA was performed to isolate liver tissues using Trizol reagent. The cDNA was obtained by using 2 μg RNA following the protocol of Transcriptor First Strand Cdna Synthesis Kit (Cat. 04897030001, Roche, Germany). In brief, 11 μL RNA diluted with water was incubated with Random Primers 1 μL and oligo (dT) primer 1 μL at 65°C for 10 min, then add 5X Reaction buffer 4 μL, RNase Inhibitor 0.5 μL, dNTPs 2 μL, Reverse Transcriptase 0.5 μL (total 20 μL) at 55°Cfor30min,andat85°Cfor5minmadeTranscriptor Reverse Transcriptase inactive. The amplification was conducted using FastStart Universal SYBR Green Master (ROX) (Cat. 049139-14001, Roche) on ABI7900 QPCR System under the conditions as follows: at 95°C for 5 min, 40 cycles at 95°C for 5 s, at 58°C for 20 s. GAPDH served as a reference gene and the data were analyzed adopting $2^{-\Delta\Delta Ct}$ method. All the primers used were listed in **Table 1**.

Western blot

Liver tissue lysate was prepared by homogenization in ice-cold RIPA Lysis Buffer (R0010, Beyotime, China) and phosphatase inhibitors (C500017, Sangon, Shanghai, China). Next, the lysates were incubated on ice for 30 min and oscillated for 30 s. After being centrifuged (10,000 g at 4°C for 30 min), the supernatant was obtained and the protein concentrations were determined using Bio-Rad protein assay kit (5000002, Bio-Rad, Hercules, CA, USA). After performing SDS-PAGE, the separated proteins were transferred onto polyvinylidenedifluoride membranes (Millipore, Billerica, CA, USA). After being blocked for 1 h, the membranes were incubated at 4°C overnight with primary antibodies as follows: anti-t-P38MAPK (1:1000, Cat. 8690, Cell Signaling Technology, Beverly, MA), anti-t-ERK (1:1000, Cat. 4695, Cell Signaling Technology), anti-p-ERK (1:1000, Cat. 4370, Cell Signaling Technology), anti-GAPDH (1:1000, Cat. 2118, Cell Signaling Technology), anti-p-P38MAPK (1:1000, Cat. 4511, Cell Signaling Technology) and anti-COX2 (1:1000, Cat. ab179800, Abcam). Next, the membranes were incubated with anti-rabbit IgG (1:5000, Cat. 7074, Cell Signaling Technology) secondary antibodies. The bands were determined by Micro chemi gel imaging system (DNR, Israel). The densitometry was determined by Quantity One (Bio-Rad) version 4.6.2.

Statistical analysis

All data were presented as mean ± SD. Graphpad Prism 5 software (GraphPad Software, San Diego, CA, USA) was used for statistical analysis. One-way analysis of variance (ANOVA) followed by Newman-Keuls test were performed. $P < 0.05$ was considered statistically significant.

Results

Berberine attenuated the tumorigenesis and reduced liver index

Combination of STZ injection and HFHC diet successfully induced tumors in mice liver in model group, while only few tumors are visible

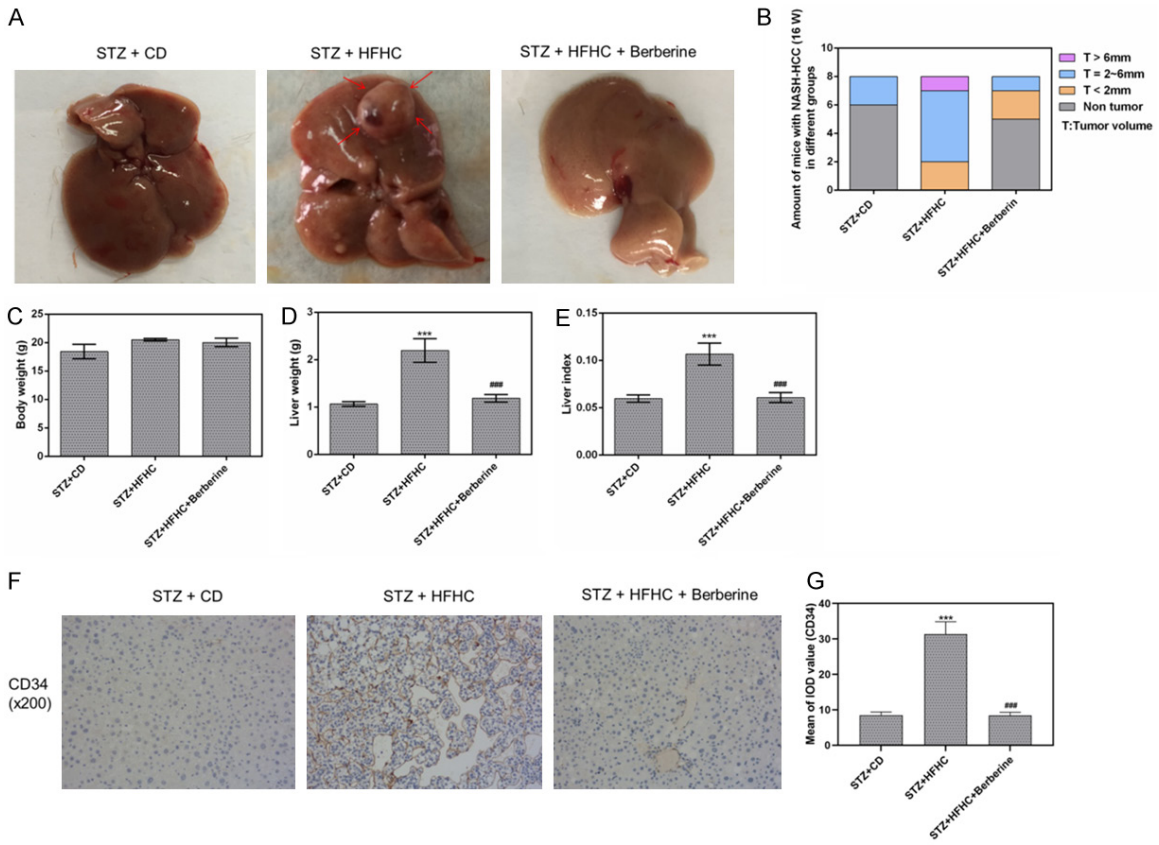

Figure 1. Berberine attenuated the tumorigenesis and reduced liver index. (A) The representative livers from mice with different treatments. The arrows represent the HCC. (B) The numbers and size of tumors in mice in the three groups. The body weight (C) and the liver weight (D) and the liver index (E). (F and G) The expression of HCC biomarker CD34 was measured by immunohistochemistry. Data are presented as the mean ± standard deviation. ***P < 0.001 versus STZ + CD group, $^{\#\#\#}$P < 0.001 versus STZ + HFHC group.

in mice treated by berberine (**Figure 1A**). The percentage of tumors at certain size range was compared among groups as shown in **Figure 1B**. Moreover, compared with STZ + CD group, the body weight of mice in both STZ + HFHC and STZ + HFHC + Berberine group increased, although with no significant difference (**Figure 1C**). We found that HFHC diet significantly increased the liver weight but little change in body weight of the mice, as a result the liver index increased significantly. However, this was reversed by berberine (**Figure 1D**, **1E**). In addition, to estimate the degree of NASH-HCC, the expression of HCC biomarker CD34 was examined. The data revealed that the staining for CD34 in model group was stronger than that in control group. The berberine administration decreased the expression of CD34 compared to model group (**Figure 1F**, **1G**).

Berberine might regulate inflammation and angiogenesis

As it was shown in Venn diagram, we identified 3622 (2897 + 725) overlapping genes from the results of pairwise comparisons conducted in Non-tumor vs. Tumor group and in Tumor vs. berberine group (P < 0.05; FC > 2 or < 0.5). Similarly, a total of 1026 (301 + 725) genes in non-tumor group and 1594 (869 + 725) genes in berberine group were evidently different from the non-tumor and tumor groups, respectively (P < 0.05; FC > 2 or < 0.5). Moreover, we found 725 intersecting genes in the three groups (P < 0.05; FC > 2 or < 0.5, **Figure 2A**). Furthermore, the core genes of these cross genes mainly fell into inflammation and angiogenesis categories (**Figure 2B**). We also found that DEGs greatly enriched in the several signaling pathways related to inflammation and

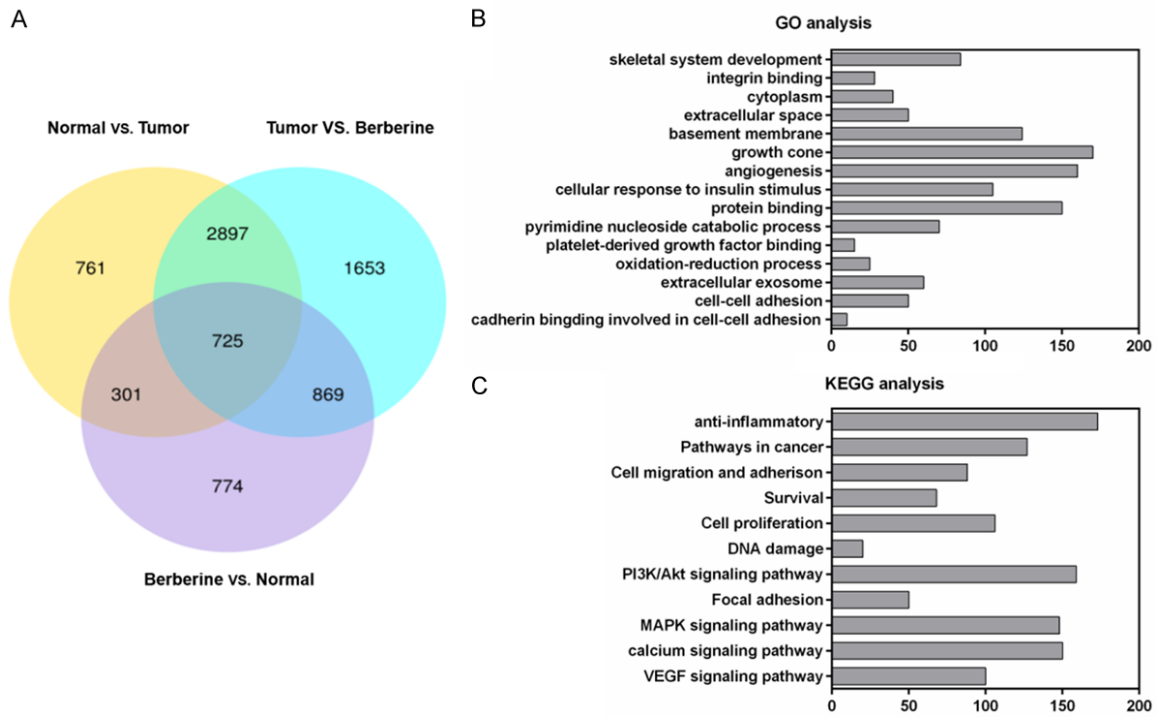

Figure 2. Effects and pathways involved in berberine-treated NASH-HCC mice by bioinformatics analysis. (A) Venn diagrams revealed the differently expressed genes in the liver tissues of nontumor, tumor and berberine groups. GO function analysis (B) and KEGG pathway enrichment analysis (C) for 725 differently expressed genes.

tumor progression by KEGG analysis (**Figure 2C**).

Berberine alleviated the liver steatohepatitis and biochemical profiles

We found that the infiltrating vacuolated cells and large confluent lipid droplets were noticeably observed in livers of mice. Steatosis, inflammation and necrosis were caused by STZ and HFHC treatment, which greatly disorganized the liver structure (**Figure 3A**). The liver steatohepatitis induced by HFHC was ameliorated by berberine. The score of steatosis ($P < 0.01$), lobular inflammation ($P < 0.01$) and NAS ($P < 0.01$) in berberine group were all lower than that in HFHC model group (**Figure 3B-E**), demonstrated that berberine mitigated NASH. Furthermore, the levels of serum ALT, AST, GLU, HDL, LDL and TC were significantly increased by STZ and HFHC diet (**Figure 3F-K**). However, high serum levels of these biochemical parameters were largely reduced by berberine.

Berberine suppressed the lipid accumulation

The NASH-HCC mice showed significant lipid accumulation in comparison to that in CD-fed mice. However, berberine was found to relieve the lipid deposition (**Figure 4A**). Meanwhile, the mRNA expressions of FASN, SCD1 and SREBP1c were up-regulated by the long-term HFHC diet, these upregulation were considerably reduced by berberine (**Figure 4B-D**).

Berberine exerted an anti-inflammatory effect

The protein of CD68 and F4/80 highly expressed in STZ-HFHC mice, while berberine significantly suppressed their expression (**Figure 5A-D**). The mRNA levels of inflammatory cytokines including IL-6, IL-1β, CD68, F4/80, MCP-1 and TNF-α were found to increase greatly in STZ-HFHC mice. The expressions of IL-6, IL-1β, MCP-1 and TNF-α were significantly lowered by berberine (**Figure 5G-J**). The effect on CD68 and F4/80 mRNA expression is relatively slight (**Figure 5E**, **5F**).

Berberine inhibited the liver fibrosis

Liver fibrosis was induced by STZ and HFHC diet. However, berberine treatment mitigated the liver fibrosis compared to STZ + HFHC group (**Figure 6A**). We also found that high expressions of liver fibrosis-associated factors α-SMA,

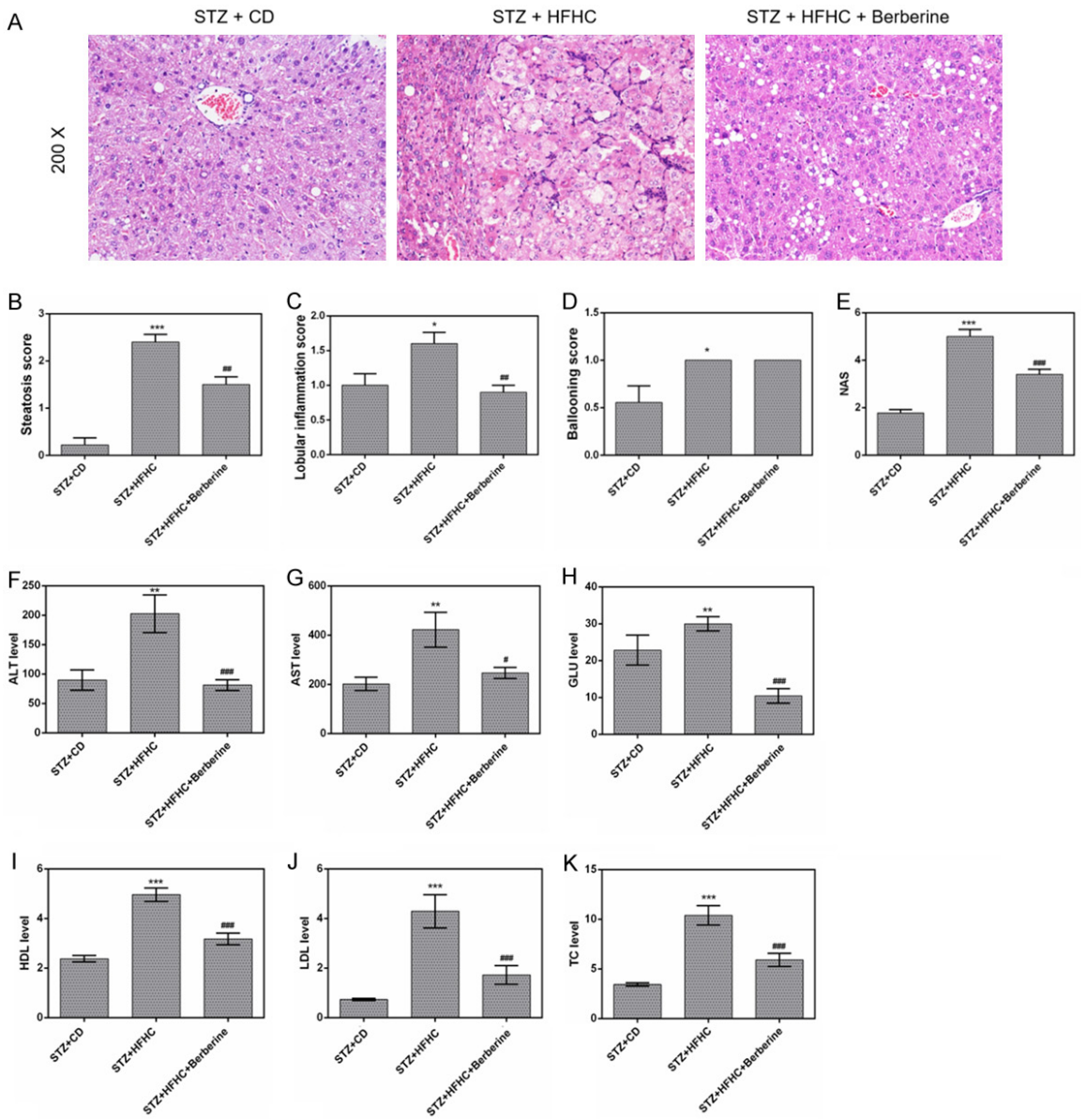

Figure 3. Berberine alleviated the liver steatohepatitis and biochemical profiles. (A) Liver sections in the three groups were stained with H&E. (B) Steatosis scores, (C) lobular inflammation scores, (D) ballooning scores and (E) NAS for the three experimental groups. The serum levels of ALT (F), AST (G), GLU (H), HDL (I), LDL (J) and TC (K) were detected using a Hitachi automatic analyser 7600. Data are presented as the mean ± standard deviation. $^{*}P < 0.05$, $^{**}P < 0.01$, $^{***}P < 0.001$ versus STZ + CD group, $^{\#}P < 0.05$, $^{\#\#}P < 0.01$, $^{\#\#\#}P < 0.001$ versus STZ + HFHC group.

COL1A1 and TIMP-1 induced by HFHC diet were remarkably decreased by berberine (**Figure 6B-D**).

Berberine prevented the angiogenic properties of HCC

The induced micro-vessels of the liver from NASH-HCC mice were found to be obviously inhibited by the berberine. Our results showed the change of CD31 and VEGF expression in three groups by immunohistochemistry (**Figure 7A-D**).

Furthermore, we also found that the mRNA expression of CD31 and VEGFR in livers of STZ-HFHC mice could be downregulated by berberine (**Figure 7E**, **7F**).

Berberine inactivated the phosphorylation of p38MAPK and ERK

In NASH-HCC mice induced by STZ and HFHC diet, the protein levels of p-p38MAPK and p-ERK were found to be remarkably increased, while the expressions of t-p38MAPK and t-ERK showed no significant difference from those in

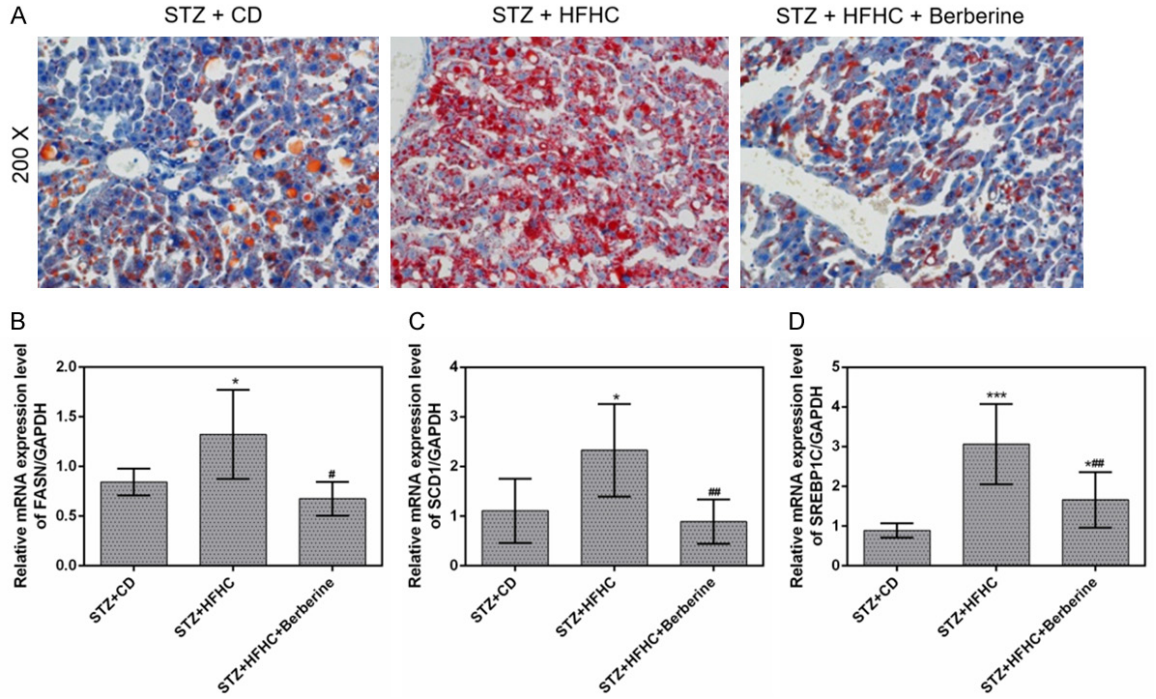

Figure 4. Berberine suppressed the lipid accumulation in liver. (A) Liver sections in the three groups were stained with Oil Red O. The mRNA expressions of FASN (B), SCD1 (C) and SREBP1c (D) in livers were measured by qPCR. Data are presented as the mean ± standard deviation. GAPDH was used as a load control. $^{*}P < 0.05$, $^{***}P < 0.001$ versus STZ + CD group, $^{\#}P < 0.05$, $^{\#\#}P < 0.01$ versus STZ + HFHC group.

STZ-CD mice. Moreover, we found that the protein levels of p-p38MAPK and p-ERK were evidently reduced by berberine (**Figure 8A**). Meanwhile, berberine obviously lowered the ratio of p-p38MAPK/t-p38MAPK in STZ-HFHC mice, by contrast, the ratio still remained at a high level in livers in STZ-HFHC mice (**Figure 8B**). Similarly, berberine was found able to lower greatly the ratio of p-ERK/t-ERK in STZ-HFHC mice (**Figure 8C**).

Berberine might alleviate NASH-HCC via p38MAPK and ERK/COX2 pathway

Phosphorylation of p38MAPK and ERK contributed to upregulation of COX2 which involved in inflammation, angiogenesis and tumor formation [21, 22]. To uncover the therapeutic mechanism of berberine in treating NASH-HCC, we determined the expression of COX2, which was a key mediator to transform inflammation to cancer, and found that COX2 mainly expressed in liver tissues with inflammatory infiltrates, nodules, HCC in model mice (**Figure 9A**, **9B**). Meanwhile, mRNA and protein expression level of COX2 declined in berberine treated mice (**Figure 9C-E**). To conclude, berberine suppressed the expression of COX2 downstream of MAPK signal pathway, suggesting berberine might inhibit inflammation and angiogenesis via p38MAPK/ERK-COX2 pathway.

Discussion

HCC is a major cause of cancer-related death. Growing evidence showed NASH has been becoming one of the most common causes of HCC. NASH can progress to HCC with/without fibrosis/cirrhosis [23]. Berberine, an isoquinoline quaternary alkaloid, derived from Coptis Rhizome, is reported as an effective drug having pharmacological properties of anti-inflammatory and anti-tumor effects [24]. While it has been shown that berberine can suppress liver tumor growth in a mouse Xenograft model and in vitro, the effects of berberine on NASH-HCC progression and the mechanisms of berberine's anti-tumor activity are still unclear. In this study, to investigate the effect of berberine on NASH-HCC, we established NASH-HCC model by injecting STZ and feeding a HFHC diet. We found that HFHC diet promoted the develop-

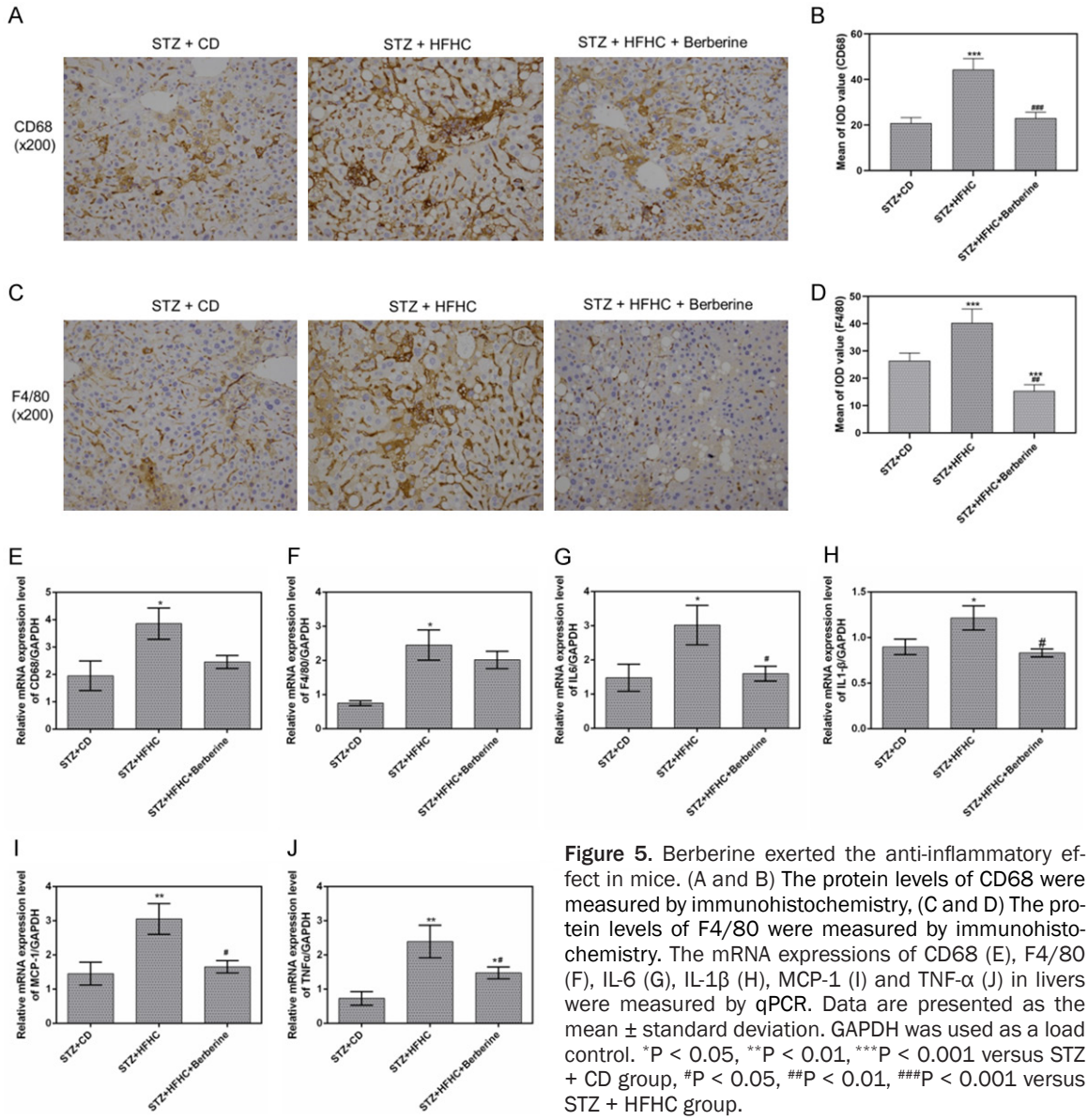

Figure 5. Berberine exerted the anti-inflammatory effect in mice. (A and B) The protein levels of CD68 were measured by immunohistochemistry, (C and D) The protein levels of F4/80 were measured by immunohistochemistry. The mRNA expressions of CD68 (E), F4/80 (F), IL-6 (G), IL-1β (H), MCP-1 (I) and TNF-α (J) in livers were measured by qPCR. Data are presented as the mean ± standard deviation. GAPDH was used as a load control. $^{*}P < 0.05$, $^{**}P < 0.01$, $^{***}P < 0.001$ versus STZ + CD group, $^{\#}P < 0.05$, $^{\#\#}P < 0.01$, $^{\#\#\#}P < 0.001$ versus STZ + HFHC group.

ment of NASH-HCC in C57BL/6J mice. Berberine ameliorates liver tumorgenesis in NASH-HCC mice.

In our previous study, we have proved that berberine can ameliorate non-alcoholic steatohepatitis in APOE$^{-/-}$ mice induced by HFHC diet [25]. In this paper, our data revealed that NAFLD activity score in NASH-HCC model mice was decreased by berberine, which is consistent with previous results. Moreover, the body weight of the animals remained relatively stable, while the liver weight as well as liver index of the animals was reduced by berberine. The levels of ALT and AST, two sensitive indicators of hepatocellular injury, clearly decreased in STZ + HFHC + berberine group. We still found that berberine evidently reduced the levels of TC, LDL and HDL in NASH-HCC mice. The results suggested that berberine could lower cholesterol and lipid. To explore the lipid-lowering effect of berberine, we examined lipogenic related genes and found that the increased expressions of FASN, SCD1 and SREBP1c in STZ-HFHC mice were significantly inhibited by berberine, suggesting that berberine might attenuate lipid accumulation.

Our GO analysis identified that berberine might be involved in inflammation and angiogenesis

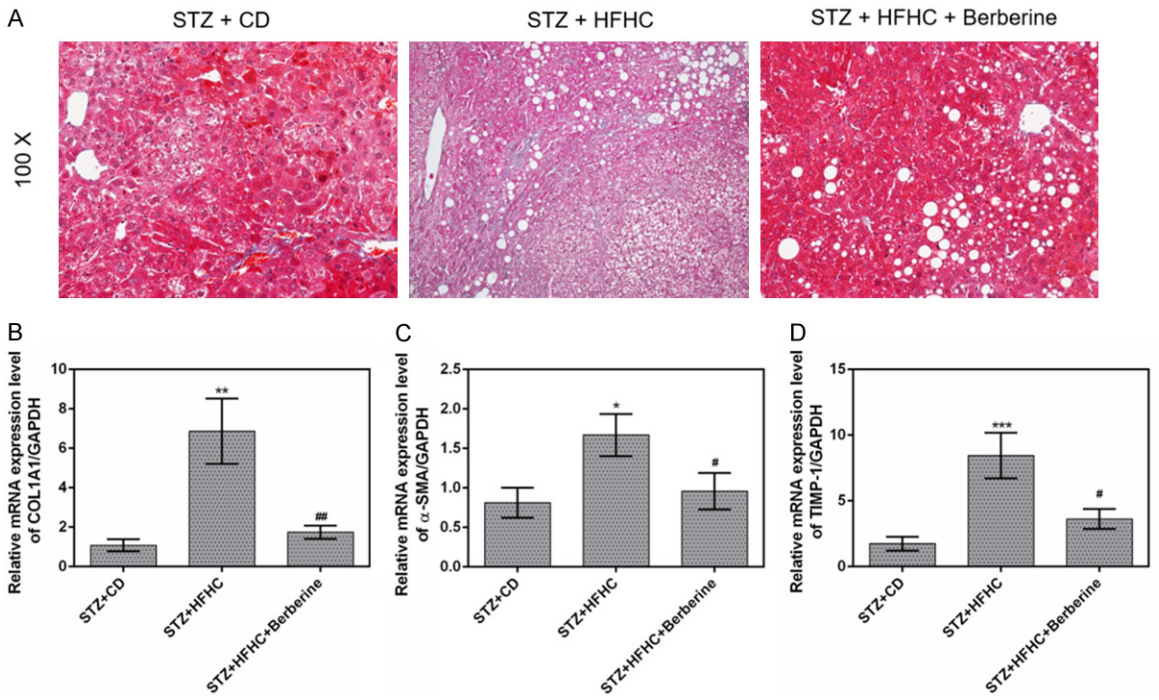

Figure 6. Berberine inhibited the liver fibrosis. (A) Liver sections in the three groups were stained with Masson staining. The mRNA expressions of Col1A1 (B), α-SMA (C) and TIMP-1 (D) in livers were measured by qPCR. Data are presented as the mean ± standard deviation. GAPDH was used as a load control. $^{*}P < 0.05$, $^{**}P < 0.01$, $^{***}P < 0.001$ versus STZ + CD group, $^{\#}P < 0.05$, $^{\#\#}P < 0.01$ versus STZ + HFHC group.

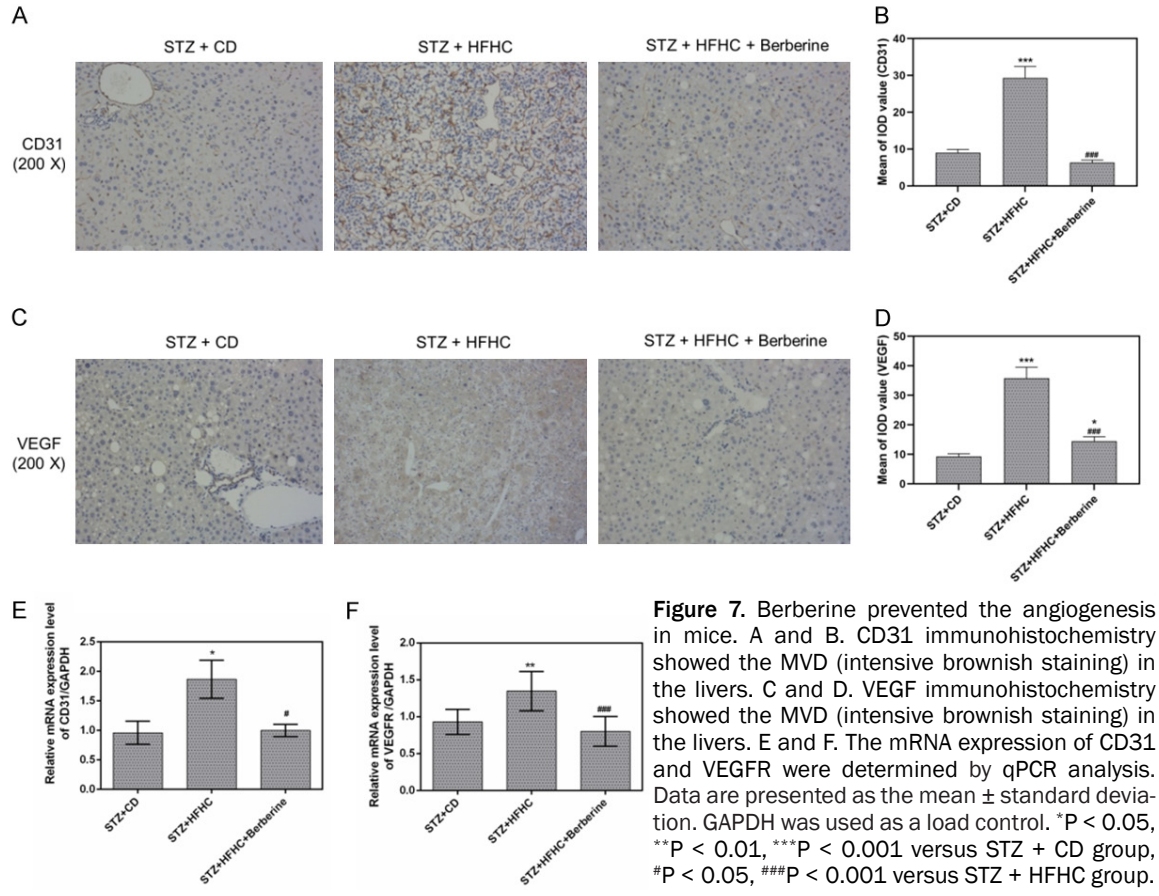

Figure 7. Berberine prevented the angiogenesis in mice. A and B. CD31 immunohistochemistry showed the MVD (intensive brownish staining) in the livers. C and D. VEGF immunohistochemistry showed the MVD (intensive brownish staining) in the livers. E and F. The mRNA expression of CD31 and VEGFR were determined by qPCR analysis. Data are presented as the mean ± standard deviation. GAPDH was used as a load control. $^{*}P < 0.05$, $^{**}P < 0.01$, $^{***}P < 0.001$ versus STZ + CD group, $^{\#}P < 0.05$, $^{\#\#\#}P < 0.001$ versus STZ + HFHC group.

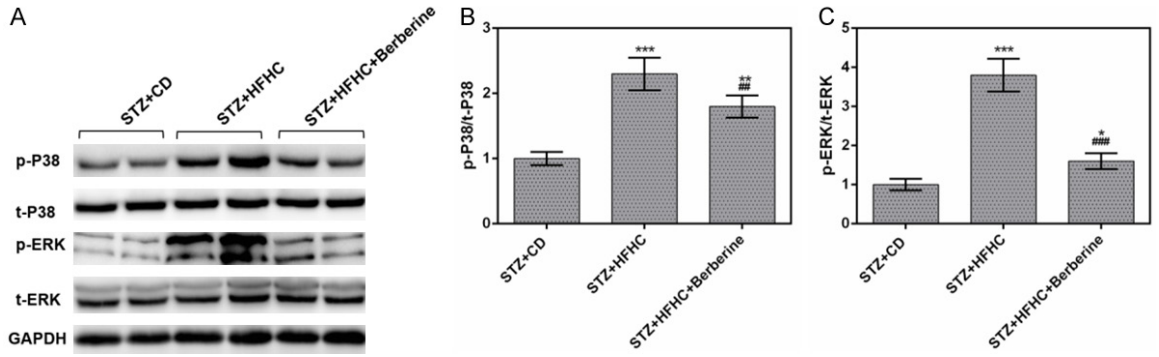

Figure 8. Berberine inactivated the phosphorylation of p38MAPK and ERK. (A) The protein levels of p-p38MAPK, p38MAPK, p-ERK and ERK were measured by performing Western blot. The ratios of p-p38MAPK/p38MAPK (B) and p-ERK/ERK (C) were significantly lowered by berberine. Data are presented as the mean ± standard deviation. GAPDH was used as a load control. $^{*}P < 0.05$, $^{**}P < 0.01$, $^{***}P < 0.001$ versus STZ + CD group, $^{\#\#}P < 0.01$, $^{\#\#\#}P < 0.001$ versus STZ + HFHC group.

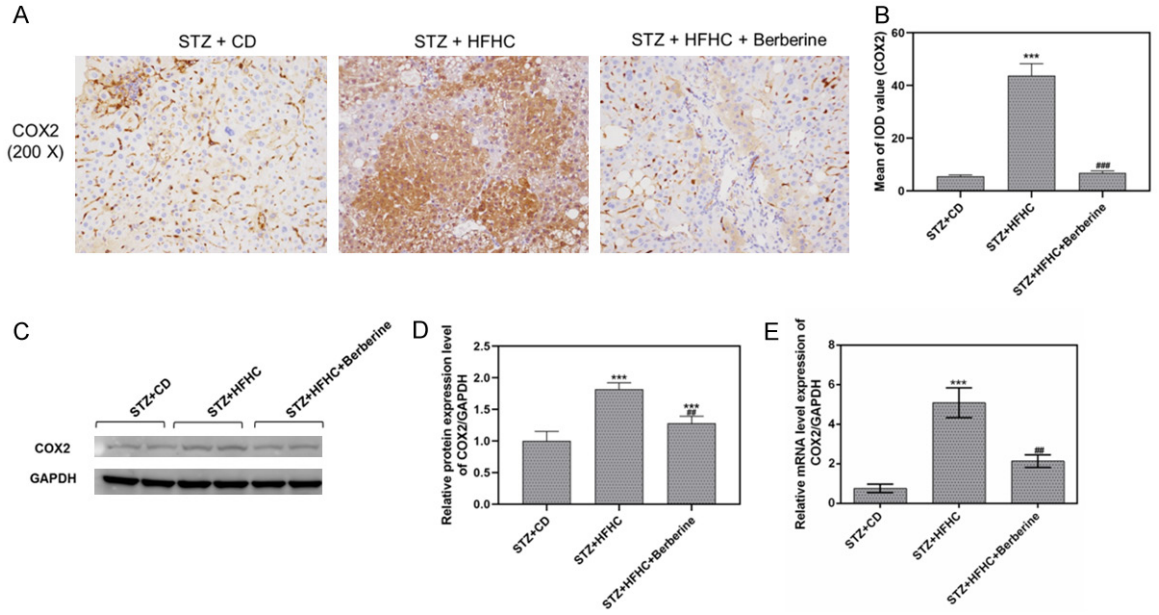

Figure 9. Berberine inhibited COX2 expression in NASH-HCC mice. A and B. The protein level of COX2 was measured by immunohistochemistry. C and D. The protein level of COX2 in livers was measured by performing Western blot. E. The mRNA level of COX2 in livers was measured by qPCR. Data are presented as the mean ± standard deviation. GAPDH was used as a load control. $^{***}P < 0.001$ versus STZ + CD group, $^{\#\#}P < 0.01$, $^{\#\#\#}P < 0.001$ versus STZ + HFHC group.

in the liver of mice. Most inflammation factors as key molecule in tumor signaling pathway involved in the transformation of inflammation to cancer, and promoted the development of cancer [26, 27]. Macrophages in the liver can promote the occurrence and development of HCC under the stimulation of long-term chronic inflammatory infiltration. Kupffer cells, as a kind of macrophages, mainly exist in the liver and can be activated when the liver is damaged. After immune activation, the Toll-like receptor on its surface binds to the ligand on the surface of the original membrane, releasing nitric oxide, arachidonic acid, hydrolase, etc., to assist in the destruction of antigens. At the same time, it also releases various cytokines, such as IL-1β, IL6, TNF-α, and MCP-1 etc. Chronic inflammatory response mediated by Kupffer cells plays an important role in the repair and regeneration of liver injury, which is directly

related to the occurrence and development of primary liver cancer. In this study, we used CD68 and F4/80 as markers of Kupffer cell activation. Immunohistochemical analysis results showed that Kupffer cells were activated obviously in the model group, and the expression of CD68 and F4/80 was decreased after berberine intervention. So were corresponding inflammatory cytokines including IL-6, IL-1β, TNF-α. The results indicated that berberine could inhibit the activation of Kupffer cells in the liver of NASH-HCC mice.

TIMP-1 has been reported to be enhanced by inflammatory cytokines [28]. Besides, TIMP1 can regulate the expression of genes associated with liver fibrosis [29]. Moreover, alpha smooth muscle actin (α-SMA) is reported to be a specific protein of myofibroblast differentiation, and collagen 1 alpha 1 (Col1A1) is highly expressed in fibrotic lung tissues [30, 31]. A recent report has revealed that berberine could inhibit over-expression of α-SMA, fibronectin, collagens I and III [32]. Additionally, berberine were corroborated to ameliorate liver fibrosis through suppressing hepatic oxidative stress and fibrogenic potential [33]. In our study, the expressions of Col1A1, α-SMA and TIMP-1 decreased in the NASH-HCC model mice that had been treated with berberine in comparison to those in the model group. This indicated that berberine could play an anti-fibrosis role in the mice.

The role of berberine being an effective anti-angiogenic agent was mainly achieved by inhibiting multiple angiogenic factors [34]. In this study, in STZ-HFHC mice, berberine was identified to greatly reduce MVD [35]. Additionally, CD31, as the prominent endothelial marker, can specifically bind to blood micro-vessels [36]. We found that in STZ-HFHC mice, the increased expressions of CD31 and VEGF were suppressed by berberine, suggesting that berberine might exert an anti-angiogenic property.

Aberrant MAPK signaling pathway activation was found able to play a critical role in the formation and progression of HCC [37]. Phosphorylation of ERK and p38MAPK involved in inflammation [38], cell proliferation [39], angiogenesis [40] and apoptosis [41]. In our study, KEGG pathway enriched analysis illustrated that p38MAPK and ERK might be related to the anti-inflammatory and anti-angiogenetic effects generated by berberine. Thus, we examined the levels of p-p38MAPK and total p38MAPK, and found that total p38MAPK level remained relatively stable, while the p-p38MAPK expression was inhibited by berberine in STZ-HFHC mice. At the same time, phosphorylation of ERK increased in STZ + HFHC group, and declined by berberine treatment. The abnormal elevated COX2 involved in inflammation, angiogenesis and promoted tumor formation [21, 22]. Phosphorylation of p38MAPK and ERK caused upregulation of COX2 in deoxycholate induced SKTG-4 esophageal cells [42]. In another NASH-HCC model induced by deoxycholic acid, COX2 overexpression was detected and conducted a pro-tumor effect by suppressing anti-tumor immunity [43]. Here, we found the increased expressions of COX2 in NASH-HCC mice were suppressed by berberine, suggesting berberine might inhibit inflammation and angiogenesis via p38MAPK/ERK-COX2 pathway. However, considering the clinical application of berberine, the elevated COX2 in NASH-HCC mice might due to the change of gut microbiota which induced by HFHC diet. Since studies have mentioned the effect of berberine on NASH through liver-gut aix [44]. Berberine might affect gut microbiota to produce multiple effects in NASH-HCC. Thus, further study are needed on this idea.

To conclude, the present study demonstrated that berberine could prevent NASH-derived HCC by producing its anti-inflammatory and anti-angiogenetic effects in mice. Moreover, the effect of berberine appeared to be related to the inhibition of COX2 via p38MAPK and ERK pathway in vivo. Thus, our results provided a potential drug for treating NASH-HCC.

Acknowledgements

This work was supported by Zhejiang Natural Science Foundation [Grant number: LQ17-H070002, LY17H030009], Hangzhou Science and Technology Bureau Project [Grant number: 20170533B42, 20180533B48], Traditional Chinese Medicine Science and Technology Project of Zhejiang Province [Grant number: 2018-ZA098], The National Natural Science Foundation of China [Grant number: 81700510, 817 = 72520, 81570524], Zhejiang Medical Science and Technology Plan [Grant number: 2018PY-039].

Disclosure of conflict of interest

None.

Address correspondence to: Junping Shi, Institute of Translational Medicine, The Affiliated Hospital of Hangzhou Normal University, No. 126 Wenzhou Road, Hangzhou 310015, Zhejiang, China. Tel: 86-571-88358063; E-mail: shijunpingab22@163.com; Weihong Ge, College of Pharmaceutical Science, Zhejiang Chinese Medical University, No. 548 Binwen Road, Binjiang District, Hangzhou 310053, Zhejiang Province, China. Tel: +86-0571-86633077; E-mail: guoweihongab22@163.com

References

[1] Ferlay J, Soerjomataram I, Dikshit R, Eser S, Mathers C, Rebelo M, Parkin DM, Forman D and Bray F. Cancer incidence and mortality worldwide: sources, methods and major patterns in GLOBOCAN 2012. Int J Cancer 2015; 136: E359-386.

[2] Younossi ZM, Koenig AB, Abdelatif D, Fazel Y, Henry L and Wymer M. Global epidemiology of nonalcoholic fatty liver disease-Meta-analytic assessment of prevalence, incidence, and outcomes. Hepatology 2016; 64: 73-84.

[3] Dyson J, Jaques B, Chattopadyhay D, Lochan R, Graham J, Das D, Aslam T, Patanwala I, Gaggar S, Cole M, Sumpter K, Stewart S, Rose J, Hudson M, Manas D and Reeves HL. Hepatocellular cancer: the impact of obesity, type 2 diabetes and a multidisciplinary team. J Hepatol 2014; 60: 110-117.

[4] Leung C, Yeoh SW, Patrick D, Ket S, Marion K, Gow P and Angus PW. Characteristics of hepatocellular carcinoma in cirrhotic and non-cirrhotic non-alcoholic fatty liver disease. World J Gastroenterol 2015; 21: 1189-1196.

[5] Chang CH, Huang WY, Lai CH, Hsu YM, Yao YH, Chen TY, Wu JY, Peng SF and Lin YH. Development of novel nanoparticles shelled with heparin for berberine delivery to treat helicobacter pylori. Acta Biomater 2011; 7: 593-603.

[6] Sun Y, Xia M, Yan H, Han Y, Zhang F, Hu Z, Cui A, Ma F, Liu Z, Gong Q, Chen X, Gao J, Bian H, Tan Y, Li Y and Gao X. Berberine attenuates hepatic steatosis and enhances energy expenditure in mice by inducing autophagy and fibroblast growth factor 21. Br J Pharmacol 2018; 175: 374-387.

[7] Jin H, Jin X, Cao B and Wang W. Berberine affects osteosarcoma via downregulating the caspase-1/IL-1beta signaling axis. Oncol Rep 2017; 37: 729-736.

[8] Xu J, Wu W, Zhang H and Yang L. Berberine alleviates amyloid beta25-35-induced inflammatory response in human neuroblastoma cells by inhibiting proinflammatory factors. Exp Ther Med 2018; 16: 4865-4872.

[9] Hesari A, Ghasemi F, Cicero AFG, Mohajeri M, Rezaei O, Hayat SMG and Sahebkar A. Berberine: a potential adjunct for the treatment of gastrointestinal cancers? J Cell Biochem 2018; 119: 9655-9663.

[10] Liu B, Fu XQ, Li T, Su T, Guo H, Zhu PL, Tse AK, Liu SM and Yu ZL. Computational and experimental prediction of molecules involved in the anti-melanoma action of berberine. J Ethnopharmacol 2017; 208: 225-235.

[11] Pan Y, Shao D, Zhao Y, Zhang F, Zheng X, Tan Y, He K, Li J and Chen L. Berberine reverses hypoxia-induced chemoresistance in breast cancer through the Inhibition of AMPK- HIF-1alpha. Int J Biol Sci 2017; 13: 794-803.

[12] Tsang CM, Cheung KC, Cheung YC, Man K, Lui VW, Tsao SW and Feng Y. Berberine suppresses Id-1 expression and inhibits the growth and development of lung metastases in hepatocellular carcinoma. Biochim Biophys Acta 2015; 1852: 541-551.

[13] Zou K, Li Z, Zhang Y, Zhang HY, Li B, Zhu WL, Shi JY, Jia Q and Li YM. Advances in the study of berberine and its derivatives: a focus on anti-inflammatory and anti-tumor effects in the digestive system. Acta Pharmacol Sin 2017; 38: 157-167.

[14] Li J, Li O, Kan M, Zhang M, Shao D, Pan Y, Zheng H, Zhang X, Chen L and Liu S. Berberine induces apoptosis by suppressing the arachidonic acid metabolic pathway in hepatocellular carcinoma. Mol Med Rep 2015; 12: 4572-4577.

[15] Fujii M, Shibazaki Y, Wakamatsu K, Honda Y, Kawauchi Y, Suzuki K, Arumugam S, Watanabe K, Ichida T and Asakura H. A murine model for non-alcoholic steatohepatitis showing evidence of association between diabetes and hepatocellular carcinoma. Med Mol Morphol 2013; 46: 141-52.

[16] Yang J, Ma XJ, Li L, Wang L, Chen YG, Liu J, Luo Y, Zhuang ZJ, Yang WJ and Zang SF. Berberine ameliorates non-alcoholic steatohepatitis in $ApoE^{-/-}$ mice. Exp Ther Med 2017; 14: 4134-4140.

[17] Tessitore A, Cicciarelli G, Vecchio FD, Gaggiano A, Verzella D, Fischietti M, Mastroiaco V, Vetuschi A, Sferra R and Barnabei R. MicroRNA expression analysis in high fat diet-induced NAFLD-NASH-HCC progression: study on C57-BL/6J mice. BMC Cancer 2016; 16: 3.

[18] Wu D, Wen W, Qi CL, Zhao RX, Lü JH, Zhong CY and Chen YY. Ameliorative effect of berberine on renal damage in rats with diabetes induced by high-fat diet and streptozotocin. Phytomedicine 2012; 19: 712-718.

[19] Zhang Q, Xiao X, Feng K, Wang T, Li W, Yuan T, Sun X, Sun Q, Xiang H and Wang H. Berberine moderates glucose and lipid metabolism through multipathway mechanism. Evid Based Complement Alternat Med 2011; 2011.
[20] Brunt EM, Kleiner DE, Wilson LA, Belt P and Neuschwander-Tetri BA. Nonalcoholic fatty liver disease (NAFLD) activity score and the histopathologic diagnosis in NAFLD: distinct clinicopathologic meanings. Hepatology 2011; 53: 810-820.
[21] Harris RE. Cyclooxygenase-2 (cox-2) and the inflammogenesis of cancer. Subcell Biochem 2007; 42: 93-126.
[22] Mobius C, Stein HJ, Spiess C, Becker I, Feith M, Theisen J, Gais P, Jutting U and Siewert JR. COX2 expression, angiogenesis, proliferation and survival in Barrett's cancer. Eur J Surg Oncol 2005; 31: 755-759.
[23] Marengo A, Rosso C and Bugianesi E. Liver cancer: connections with obesity, fatty liver, and cirrhosis. Annu Rev Med 2016; 67: 103-17.
[24] Sun Y, Xun K, Wang YT and Chen XP. A systematic review of the anticancer properties of berberine, a natural product from Chinese herbs. Anti-Cancer Drugs 2009; 20: 757.
[25] Yang J, Ma XJ, Li L, Wang L, Chen YG, Liu J, Luo Y, Zhuang ZJ, Yang WJ and Zang SF. Berberine ameliorates non-alcoholic steatohepatitis in $ApoE^{-/-}$ mice. Exp Ther Med 2017; 14: 4134-4140.
[26] Sun B and Karin M. Obesity, inflammation and liver cancer. J Hepatol 2012; 56: 704.
[27] Stauffer JK, Scarzello AJ, Jiang Q and Wiltrout RH. Chronic inflammation, immune escape, and oncogenesis in the liver: a unique neighborhood for novel intersections. Hepatology 2012; 56: 1567-1574.
[28] Arendt E, Ueberham U, Bittner R, Gebhardt R and Ueberham E. Enhanced matrix degradation after withdrawal of TGF-beta1 triggers hepatocytes from apoptosis to proliferation and regeneration. Cell Prolif 2010; 38: 287-299.
[29] Wang K, Lin B, Brems JJ and Gamelli RL. Hepatic apoptosis can modulate liver fibrosis through TIMP1 pathway. Apoptosis 2013; 18: 566-577.
[30] Hu M, Che P, Han X, Cai GQ, Liu G, Antony V, Luckhardt T, Siegal GP, Zhou Y and Liu RM. Therapeutic targeting of SRC kinase in myofibroblast differentiation and pulmonary fibrosis. J Pharmacol Exp Ther 2014; 351: 87-95.
[31] Huang M, Wang YP, Zhu LQ, Cai Q, Li HH and Yang HF. MAPK pathway mediates epithelial-mesenchymal transition induced by paraquat in alveolar epithelial cells. Environ Toxicol 2016; 31: 1407-1414.
[32] Chitra P, Saiprasad G, Manikandan R and Sudhandiran G. Berberine inhibits smad and non-Smad signaling cascades and enhances autophagy against pulmonary fibrosis. J Mol Med (Berl) 2015; 93: 1015-31.
[33] Domitrović R, Jakovac H, Marchesi VV and Blažeković B. Resolution of liver fibrosis by isoquinoline alkaloid berberine in CCl_4-intoxicated mice is mediated by suppression of oxidative stress and upregulation of MMP-2 expression. J Med Food 2013; 16: 518-28.
[34] Hamsa TP and Kuttan G. Antiangiogenic activity of berberine is mediated through the downregulation of hypoxia-inducible factor-1, VEGF, and proinflammatory mediators. Drug Chem Toxicol 2012; 35: 57-70.
[35] Nadkarni NJ, Geest KD, Neff T, Young BD, Bender DP, Ahmed A, Smith BJ, Button A and Goodheart MJ. Microvessel density and p53 mutations in advanced-stage epithelial ovarian cancer. Cancer Lett 2013; 331: 99.
[36] Al-Ghorbani M, Vigneshwaran V, Ranganatha VL, Prabhakar BT and Khanum SA. Synthesis of oxadiazole-morpholine derivatives and manifestation of the repressed CD31 Microvessel Density (MVD) as tumoral angiogenic parameters in Dalton's lymphoma. Bioorg Chem 2015; 60: 136-46.
[37] Kaminska B. MAPK signalling pathways as molecular targets for anti-inflammatory therapy--from molecular mechanisms to therapeutic benefits. Biochim Biophys Acta 2005; 1754: 253-262.
[38] Yuan Z, Matias FB, Wu J, Liang Z and Sun Z. Koumine attenuates lipopolysaccaride-stimulated inflammation in RAW264.7 macrophages, coincidentally associated with inhibition of NF-kappaB, ERK and p38 pathways. Int J Mol Sci 2016; 17: 430.
[39] Guo K, Liu Y, Zhou H, Dai Z, Zhang J, Sun R, Chen J, Sun Q, Lu W, Kang X and Chen P. Involvement of protein kinase C beta-extracellular signal-regulating kinase 1/2/p38 mitogen-activated protein kinase-heat shock protein 27 activation in hepatocellular carcinoma cell motility and invasion. Cancer Sci 2008; 99: 486-496.
[40] Chao TH, Tseng SY, Li YH, Liu PY, Cho CL, Shi GY, Wu HL and Chen JH. A novel vasculo-angiogenic effect of cilostazol mediated by cross-talk between multiple signalling pathways including the ERK/p38 MAPK signalling transduction cascade. Clin Sci (Lond) 2012; 123: 147-159.
[41] Li S, Zhong M, Yuan Y and Zhang L. Differential roles of p38 MAPK and ERK1/2 in angiopoietin-2-mediated rat pulmonary microvascular endothelial cell apoptosis induced by lipopoly-

saccharide. Exp Ther Med 2018; 16: 4729-4736.
[42] Looby E, Abdel-Latif MM, Athie-Morales V, Duggan S, Long A and Kelleher D. Deoxycholate induces COX-2 expression via Erk1/2-, p38-MAPK and AP-1-dependent mechanisms in esophageal cancer cells. BMC Cancer 2009; 9: 190.
[43] Loo TM, Kamachi F, Watanabe Y, Yoshimoto S, Kanda H, Arai Y, Nakajima-Takagi Y, Iwama A, Koga T, Sugimoto Y, Ozawa T, Nakamura M, Kumagai M, Watashi K, Taketo MM, Aoki T, Narumiya S, Oshima M, Arita M, Hara E and Ohtani N. Gut microbiota promotes obesity-associated liver cancer through PGE2-mediated suppression of antitumor immunity. Cancer Discov 2017; 7: 522-538.
[44] Cao Y, Pan Q, Cai W, Shen F, Chen GY, Xu LM and Fan JG. Modulation of Gut Microbiota by berberine improves steatohepatitis in high-Fat Diet-Fed BALB/C mice. Arch Iran Med 2016; 19: 197-203.